Predeployment of Regenerators for Fast Service Provisioning in DWDM Transport Networks [Invited]

João Pedro

***Abstract*—Dense wavelength division multiplexing (DWDM) transport networks are evolving to support dynamic setup/teardown of wavelength services. This is becoming possible mainly via node architectures with flexible add/drop port utilization, where an already deployed transponder can be tuned to any wavelength and configured to transmit/receive via any output/input direction, and advanced control and management software, which provide the means to remotely reconfigure equipment end to end. In long-haul networks, exploiting these capabilities to quickly set up new services also demands that 3R regenerators (performing reamplification, reshaping, and retiming) have been deployed in advance. This paper proposes a framework that, first, characterizes stochastically the fitness of each network node as a placeholder for predeployed regenerators based on the network and traffic information available and, second, distributes the set of regenerators to match as closely as possible the fitness values. Network simulation on a reference long-haul network under dynamic traffic is used to evaluate the effectiveness of four fitness estimation strategies, each based on a different set of forecasts about the expected network operating conditions. The results highlight that when the main assumptions embedded in these strategies hold during network operation significant benefits can be attained, in terms of lower service blocking probability and/or reduced number of predeployed 3R regenerators, by exploiting additional information when computing the node's fitness values.**

***Index Terms*—Network optimization; Regenerator placement; Wavelength routing; WDM networks.**

I. Introduction

The recent progress toward highly flexible dense wavelength division multiplexing (DWDM) transport networks, such as the availability of colorless, directionless, contentionless (CDC) reconfigurable optical add/drop multiplexer (ROADM) nodes [1], transponder technology and design options to support beyond 100 Gb/s optical channels [2], and advanced control and management software [3], is setting the stage for fast service setup in these networks. Particularly, CDC ROADMs, and to a lesser extent noncontentionless architectures, are essential for configuring on demand already deployed transponders and regenerators to support new wavelength services without constraints related to using a specific wavelength channel and input/output direction (degree) of the node, thereby avoiding manual interventions to reconnect these devices to another add/drop port [4]. Moreover, with the prospects of deploying software-defined networking solutions in transport networks, an appropriate tool set for dynamically controlling, managing, and optimizing a multilayer, multidomain, and multivendor network can finally become available [3]. Combined, these developments on both the hardware and software side can support enhanced service provisioning in transport networks. This opportunity, along with the new business models enabled by it, is already being envisioned by major network operators [5], which can take advantage of a reduced wavelength service setup time and of minimizing the number of truck rolls required to deploy reamplification, reshaping, and retiming (3R) regenerators in long-haul networks, provided that transponders and regenerators have been predeployed.

Transponders and 3R regenerators are expensive devices, accounting for a large share of the total cost of deploying and operating a transport network [6,7]. And while it is straightforward to determine the number of transponders needed to establish a wavelength service (one at each end node), the number of 3R regenerators depends on a wider range of factors, such as the optical performance of the line interface and the routing, wavelength assignment, and 3R placement algorithms. Consequently, a significant amount of work on optimizing the deployment of 3R regenerators in transport networks has been reported, addressing different problems. For instance, [8] describes and compares several algorithms to place the minimum number of 3Rs along the path of a service to minimize the blocking of forthcoming services, whereas [9] analyzes the problem of jointly optimizing regenerator placement and grooming lower rate client signals. Several works have studied the scenario where only a subset of network sites have predeployed regenerators. Particularly, [10] proposes heuristic methods to select which sites should be part of the subset, assuming a predefined subset size, whereas [11] proposes strategies to minimize the number of sites where regenerators should be predeployed, so as to reduce the operational expenditures related to installing additional 3R regenerators.

Manuscript received July 2, 2014; revised September 24, 2014; accepted October 12, 2014; published November 13, 2014 (Doc. ID 215210).

J. Pedro is with Coriant Portugal, Rua Irmãos Siemens 1-1A, 2720-093 Amadora, Portugal, and is also with the Instituto de Telecomunicações, Instituto Superior Técnico, Av. Rovisco Pais 1, 1049-001 Lisboa, Portugal (e-mail: joao.pedro@coriant.com).

http://dx.doi.org/10.1364/JOCN.7.00A190

Under the assumption that the DWDM network has all the required functionalities to provide fast wavelength service provisioning and that a set of regenerators can be deployed prior to network operation, another dimensioning problem is to determine how these regenerators should be distributed over the network nodes. In [12] an analytical model is proposed to predict the share of 3R regenerators at each node. It exploits two factors, the relative position of the node in the network topology and the length of the links connected to it, but to maintain tractability of the problem neglects relevant factors, such as the length of all other links and the traffic pattern to be supported. The work in [13] assumes transponder/regenerator usage at a given node tends to follow a chi-squared distribution with a certain number of degrees of freedom. It uses this estimation to calculate the number of these devices that should be placed at the node to attain a target blocking probability due to lack of free transponders/regenerators. However, it requires intensive network simulations and an accurate knowledge of the traffic demands to calculate for each node the number of degrees of freedom of the chi-squared distribution.

The seminal work reported by the author in [14] proposes an alternative approach to determine how 3R regenerators should be distributed over the network nodes to optimize their utilization. It comprises a stochastic framework to estimate the fitness of each node as a placeholder for 3R regenerators and distribute a limited set of regenerators to be predeployed according to their fitness values.

This paper provides a more detailed description of the novel stochastic 3R regenerator predeployment framework and a more extensive performance analysis of the different fitness computation strategies introduced in [14]. Network simulation on a reference long-haul DWDM network shows that improved performance, in the form of reduced service blocking probability and smaller number of predeployed regenerators to meet a target service blocking probability, can be attained when embedding more traffic and routing related forecasts in the fitness estimation process. However, it also hints that realizing such benefits depends on the extent of the eventual mismatches between the assumptions exploited when planning the regenerators' predeployment and the conditions observed during network operation.

This paper is organized as follows. Section II introduces the network scenario under investigation and describes a set of strategies to estimate the fitness of each node as a placeholder for 3R regenerators, as well as an algorithm to distribute a set of predeployed regenerators by the nodes to match as closely as possible their fitness values. Section III presents a comprehensive study of the performance impact of the different fitness computation strategies when used for planning the predeployment of regenerators in a reference long-haul DWDM network. Finally, the main conclusions of this work are highlighted in Section IV.

II. Stochastic Framework for 3R Regenerator Predeployment

The number of 3R regenerators predeployed in a DWDM transport network is key to successfully supporting fast service provisioning and reducing additional truck rolls. On the one hand, a sufficiently large number of these devices should be present to minimize the probability of wavelength service blocking due to lack of one or more regenerators. On the other hand, 3R regenerators are an expensive resource and, as a result, operators want to limit as much as possible the number of devices that need to be acquired. Hence, planning the predeployment of a limited set of regenerators should target distributing them across the DWDM network in such a way that their utilization during operation is maximized.

This section starts by modeling the network scenario under investigation. Subsequently, it describes the concept of assigning a fitness value to each node to quantify how it is expected to compare with other nodes as a placeholder for 3R regenerators, and it details four different strategies to compute fitness. Furthermore, it presents an algorithm to solve the problem of distributing a discrete number of regenerators over the nodes so as to match their fitness values.

A. Network Scenario

The network scenario considered in this work assumes the operator of a long-haul transport network designed to support dynamically switched wavelength services has to predeploy a set of transponders and regenerators at the network nodes prior to the start of operation. The total number of devices to be predeployed can be computed, for example, based on traffic estimations and/or budget restrictions of the network operator. The specific strategy used to determine the size of the set of transponders and regenerators is outside the scope of this work. Consider that the DWDM network has a total of N ROADM nodes and L bidirectional fiber links, each carrying up to W wavelength channels. Each ROADM node i has a nodal degree $M(i)$ and, by default, has the general architecture depicted in Fig. 1. It consists of a CDC ROADM [4] and a set of $n_{\mathrm{TP}}(i)$ predeployed transponders along with a set of $n_{\mathrm{3R}}(i)$ predeployed 3R regenerators. Both the transponders and regenerators are equipped with line interfaces tunable across the entire C band. A total of $n_{\mathrm{TP}}^{\mathrm{total}}$ transponders and a total of $n_{\mathrm{3R}}^{\mathrm{total}}$ 3R regenerators are to be predeployed in the DWDM network. These correspond to a transponder count and a regenerator count normalized to the maximum number of line interfaces that can be deployed as given in Eqs. (1) and (2), respectively. Noteworthily, each 3R regenerator occupies two add/drop ports since it requires two line interfaces.

In the following, the normalized transponder count and the normalized regenerator count are computed assuming each node can have full add/drop port capacity; that is, there is up to one add/drop port per input/output channel of the ROADM. Therefore, the total number of add/drop ports that can be used to install line interfaces at node i is given by Eq. (3):

$$r_{\mathrm{TP}} = \frac{\sum_{i=1}^{N} n_{\mathrm{TP}}(i)}{\sum_{i=1}^{N} n_{\mathrm{AD}}(i)}, \quad \text{with} \sum_{i=1}^{N} n_{\mathrm{TP}}(i) = n_{\mathrm{TP}}^{\mathrm{total}}, \tag{1}$$

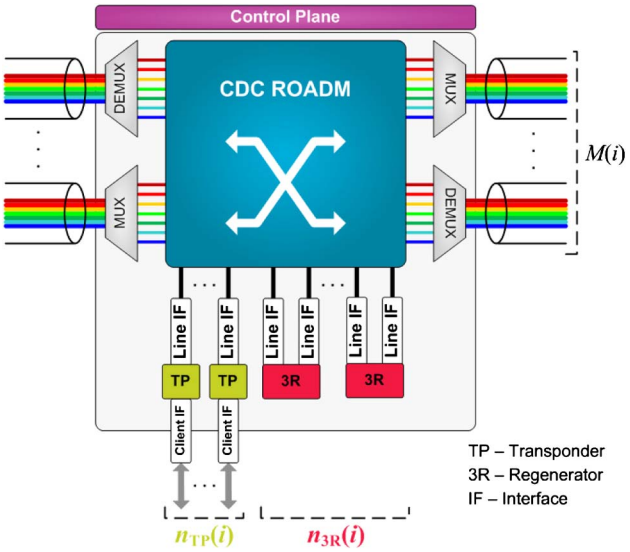

Fig. 1. Transport node architecture with separate line interfaces for transponders and regenerators.

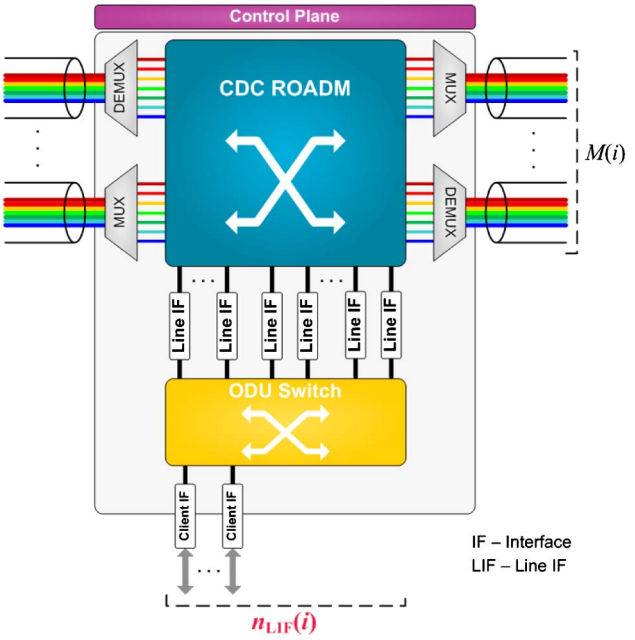

Fig. 2. Transport node architecture with common line interfaces for transponders and regenerators.

$$r_{3R} = \frac{\sum_{i=1}^{N} 2 \cdot n_{3R}(i)}{\sum_{i=1}^{N} n_{AD}(i)}, \quad \text{with} \sum_{i=1}^{N} n_{3R}(i) = n_{3R}^{\text{total}}, \tag{2}$$

$$n_{AD}(i) = W \cdot M(i), \qquad 1 \le i \le N. \tag{3}$$

The default node architecture assumes transponders and regenerators are separate devices, each having its own line interfaces and, in the case of transponders, its own client interfaces. An alternative transport node design, illustrated in Fig. 2, includes an electrical switch, acting at the optical-channel data unit (ODU) sublayer, between the client and line interfaces [15]. The ODU switch can connect a client interface to a line interface (i.e., transponder functionality) or can connect two line interfaces (i.e., regenerator functionality). With this architecture, the same line interface can be used in nonoverlapping time intervals to realize the functionality of a transponder or regenerator, further improving resource utilization in a dynamic service provisioning scenario. For modeling purposes and assuming that at the planning stage the individual fractions of line interfaces intended for usage primarily as transponders and regenerators are still given (albeit they are shared for both functionalities during operation) the line interface count is obtained from these values as given by Eq. (4):

$$n_{LIF}(i) = 2 \cdot n_{3R}(i) + n_{TP}(i), \qquad 1 \le i \le N. \tag{4}$$

The analysis of Section III considers both the default node architecture with separate line interfaces for transponders and regenerators and the alternative node architecture with common line interfaces to realize these functionalities.

B. Strategies for 3R Fitness Computation

The first stage of the stochastic-based framework for 3R regenerator placement consists of using available network, traffic, and routing information/forecasts to estimate the fitness of each node i as a placeholder for 3R regenerators, which can be represented as a probability density function (PDF), denoted as $\text{pdf}_{3R}(i)$. In a Greenfield deployment, the strategies utilized to estimate the node's fitness can rely on characteristics of the network topology and, eventually, on the routing paths that are likely to be utilized between each node pair and the expected optical performance of the line interface technology to be deployed. Additionally, they may also exploit estimations regarding the spatial distribution of the traffic demands, but only if the network operator has them and finds them to be reliable. Figure 3 illustrates four different strategies to compute the node's fitness embedding increasingly more sources of information into the estimation process. In the following, these strategies are detailed.

Table I summarizes the expressions used to compute the fitness value, $\text{pdf}_{3R}(i)$, for each of the four strategies and also gives insight on their complexity by estimating the number of operations involved in the computation. The simplest uniform strategy consists of assigning the same fitness value to every node in the network. According to this strategy, there is no differentiation between nodes, and all of them are considered to be equally good candidates to be placeholders of predeployed 3R regenerators. The nodal degree strategy introduces a simple differentiation criterion between nodes by setting the fitness value to be directly proportional to the nodal degree. The rationale is that nodes with higher nodal degree are expected to be traversed by a larger number of traffic demands. Since

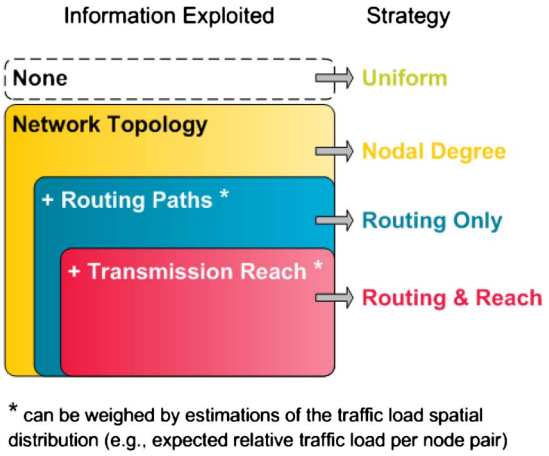

Fig. 3. Strategies for 3R node fitness computation.

some transit traffic demands may need 3R regeneration at this particular node, a larger number of transit traffic demands is assumed to translate into an increase in the average number of requests for 3R regeneration during dynamic network operation.

The nodal degree strategy only hints at the amount of transit traffic demands based on the number of fiber links that start or end at the node, thus neglecting the geographical positioning of the node and the actual routing paths that will be utilized to route traffic demands. The routing only strategy attempts to more accurately model the average number of transit traffic demands via a preoperation exercise that consists of computing the set of shortest paths between nodes using a given path computation metric Q, $\Pi_{SP}(Q)$. Importantly, the routing metric, which can be, for example, hop count or distance, should match the one that will be used during network operation. Node i is considered to be a transit node for traffic demands between nodes s and d if it is contained in path $\pi(s,d) \in \Pi_{SP}(Q)$. As a result of applying this strategy, a node that is traversed by a larger number of shortest paths is assigned a higher fitness value.

Finally, instead of estimating fitness solely via the amount of transit traffic demands, the routing and reach strategy also exploits the transmission reach of the line interface technology to be deployed to pinpoint at which nodes of a given routing path 3R regeneration is expected to be performed. This is accomplished by first calculating for every shortest path $\pi(s,d)$ all feasible combinations of 3R regenerator placements that require the minimum number of 3Rs and then creating the set of transit nodes that are utilized by at least one of these regenerator placement combinations over $\pi(s,d)$, denoted as $P_{\min}(\pi(s,d))$. Using these sets it is possible to estimate for each node i the total number of shortest paths that traverse it and are likely to utilize the node to realize 3R regeneration. Consequently, a node prone to be utilized for 3R regeneration by a larger number of shortest paths is assigned a higher fitness value.

In the absence of traffic demand estimations, the routing only and routing and reach strategies can be used

TABLE I
PDF (Fitness) and Estimated Complexity

Strategy	3R PDF	Complexity
Uniform	$\text{pdf}_{3R}(i) = 1/N$	$O(1)$
Nodal degree	$\text{pdf}_{3R}(i) = M(i)/2L$	$O(N)$
Routing only	$\text{pdf}_{3R}(i) = T(i)/\sum_{s,d}\lvert\pi(s,d)\rvert - 2$, where $T(i) = \sum_{s,d}\{1 : i \in \pi(s,d)\backslash\{s,d\}\}$	$O(N^3)^a$
Routing & reach	$\text{pdf}_{3R}(i) = R(i)/\sum_{s,d}\lvert P_{\min}(\pi(s,d))\rvert$, where $R(i) = \sum_{s,d}\{1 : i \in P_{\min}(\pi(s,d))\}$	$O(N^3 \cdot f(x))^b$

[a]Using for every node Dijkstra's algorithm to compute the shortest path to all other nodes.
[b]Using for every node Dijkstra's algorithm to compute the shortest path to all other nodes and calculating for each shortest path all combinations of 3R placements that require the minimum number of 3Rs (assumed to have complexity $f(x)$).

assuming all node pairs are equally likely to exchange traffic. In case traffic demand estimations exist, they can be exploited to refine the fitness figures. Let $\gamma(s,d)$ be the expected average traffic load offered between nodes s and d. The expressions used to compute $\text{pdf}_{3R}(i)$, as given in Table I, simply need to be updated such that the contribution of each routing path $\pi(s,d)$, traversing the node (routing only) or on which the node is likely to be used for 3R regeneration (routing and reach), is no longer unitary but instead the value of $\gamma(s,d)$.

Noteworthily, embedding more information into the fitness estimation process also means more assumptions are being made regarding the operating conditions, some of which may not hold during network operation. Section III also presents results for scenarios where there are mismatches between the assumptions made when predeploying the 3R regenerators and the actual conditions of operation.

C. Algorithm for Minimum 3R Fitness Deviation

The second stage of the stochastic-based framework for 3R regenerator placement comprises the distribution of the set of n_{3R}^{total} regenerators over the network nodes. Ideally, the set of regenerators is distributed by the N nodes such that the computed PDF is exactly matched, that is, is given by Eq. (5):

$$\text{pdf}_{3R}(i) = n_{3R}(i)/n_{3R}^{\text{total}}, \qquad 1 \le i \le N. \tag{5}$$

In view of the discrete nature of variables $n_{3R}(i)$, the abovementioned matching of target and actual PDFs of the predeployed regenerators may not be possible in practice. Hence, the 3R regenerators should be distributed over the network nodes to match as closely as possible their fitness values. This can be modeled as an optimization problem whose objective function consists of minimizing the overall deviation between the target and actual PDFs. A mixed integer linear programming (MILP) formulation to model and solve this problem is given in Appendix A. However, since solving the MILP model for large networks may be computationally intensive, a heuristic algorithm for

TABLE II
GREEDY ALGORITHM TO MINIMIZE 3R FITNESS DEVIATION

(S1)	Initialize the 3R counter of each node i, that is, $n_{3R}(i) = 0$ for $1 \le i \le N$. Initialize the iteration counter, $j = 1$.
(S2)	For each node i, update the deviation between the target fitness and the current 3R distribution, as given by $$\Delta\text{pdf}_{3R}(i) = \text{pdf}_{3R}(i) - n_{3R}(i)/n_{3R}^{\text{total}}. \quad (6)$$
(S3)	For the placement of the next predeployed 3R, select the node $i*$ with largest deviation from the expected PDF and which still has free add/drop ports to support the additional 3R, that is, $$i* = \arg\max_i \{\Delta\text{pdf}_{3R}(i) : n_{TP}(i) + 2n_{3R}(i) \le n_{AD}(i) - 2\}. \quad (7)$$
(S4)	Update the number of predeployed 3Rs at node $i*$, $n_{3R}(i*) \leftarrow n_{3R}(i*) + 1$.
(S5)	In case there are unplaced 3Rs, that is, $j < n_{3R}^{\text{total}}$, increment the iteration counter, $j \leftarrow j + 1$, and repeat (S2). Otherwise, all predeployed 3Rs have been placed, and the algorithm ends.

quickly distributing the set of n_{3R}^{total} regenerators to minimize the deviation between the target PDF and the real one is described in Table II.

The algorithm executes a total of n_{3R}^{total} iterations, where each iteration consists of allocating one of the regenerators to be predeployed to the network node which currently has the largest gap between the expected and real values of the PDF. This greedy approach enables the following to be guaranteed: (1) nodes ranked higher as placeholders for regenerators are the first ones to receive predeployed 3Rs, and (2) in the end of the algorithm execution, the number of predeployed regenerators at a node is closely proportional to its fitness value, that is, nodes with higher $\text{pdf}_{3R}(i)$ tend to be assigned a larger number of predeployed 3Rs.

As a final remark, albeit the stochastic-based framework for regenerator predeployment is described here for usage in a Greenfield network deployment scenario, the proposed framework can also be adapted for the case of a long-haul transport network already providing dynamically switched wavelength services (Brownfield scenario). Particularly, if at a given point in time, the network operator plans to deploy one or several additional 3Rs, he could exploit statistics of past services set up in the network to better estimate the fitness values with both the routing only and the routing and reach strategies.

III. RESULTS AND DISCUSSION

In the following, an assessment of the expected blocking performance of a long-haul DWDM transport network with predeployed transponders and regenerators and supporting fast setup of wavelength services is presented.

This section describes the simulation setup implemented to compute the wavelength service blocking probability and presents simulation results for three main scenarios. In the first one there is a matching between the traffic and routing conditions used as input for planning the predeployment of 3R regenerators and the ones observed during operation, whereas the second scenario challenges some of these assumptions during operation. Finally, the last scenario assesses the impact of having common line interfaces instead of separate ones for transponders and regenerators.

A. Simulation Setup

The U.S. CORONET CONUS topology [16], illustrated in Fig. 4, is used in the performance evaluation via network simulation. This reference long-haul network has $N = 75$ ROADM nodes and $L = 99$ bidirectional fiber links. Each fiber link is assumed to carry $W = 96$ wavelength channels, and each channel is operated at a data rate $\mu = 100$ Gb/s. A normalized transponder count $r_{TP} = 0.20$ is utilized, unless stated otherwise, and predeployed transponders are always uniformly distributed over the 75 nodes. The normalized regenerator count r_{3R} is varied between 0.02 and 0.26 with increments of 0.02.

The randomly generated traffic demands are uniformly distributed among a subset of half of all node pairs, and both the traffic demand duration and interarrival time are exponentially distributed. The average offered traffic load normalized to the network capacity is given by Eq. (8), where $h(s,d)$ is the hop count of the shortest path between nodes s and d. Network planning assumes distance is the path computation metric. For simplicity, optical performance is modeled by imposing a maximum transmission reach of 2000 km and a 60 km penalty per node traversed [4]. The average service blocking probability is computed from 10 independent simulation runs:

$$\Gamma_{\text{net}} = \frac{\sum_{s,d} \gamma(s,d) \cdot h(s,d)}{\mu \cdot W \cdot 2L}. \quad (8)$$

In order to better understand the impact of the fitness computation strategies in the distribution of predeployed 3R regenerators, Figs. 5 and 6 show for $r_{3R} = 0.12$ how 3R regenerators are distributed across the network when the different strategies are used. As can be observed, with

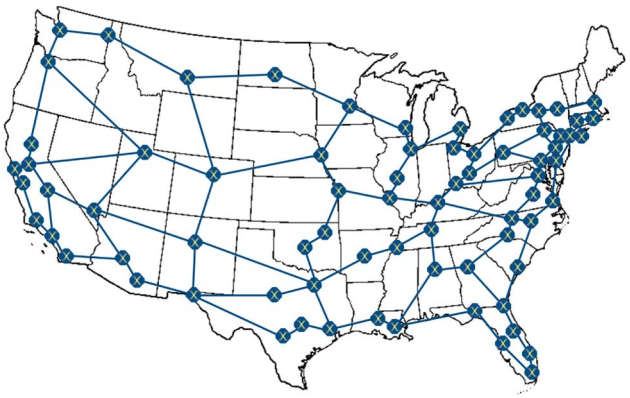

Fig. 4. 75-node CORONET CONUS topology.

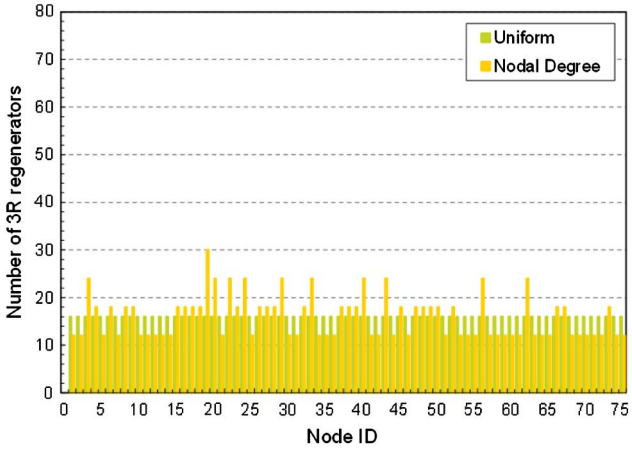

Fig. 5. Distribution of 3R regenerators for $r_{3R} = 0.12$ using the uniform and nodal degree strategies.

the uniform strategy all nodes have approximately the same number of regenerators, whereas with nodal degree the ratio between the nodes with more 3R regenerators and the ones with fewer regenerators is determined by the maximum and minimum nodal degrees (5/2 in this network topology). This corresponds to a modest variance in the number of regenerators per node when comparing it to that obtained with both routing only and routing and reach strategies, according to which some network nodes should be assigned a large number of regenerators, while others should have few or even none. The highest variance in the 3R regenerator distribution is obtained when utilizing the routing and reach strategy.

B. Matching Between Planning and Operation

The first set of simulation results considers that the assumptions done when predeploying the regenerators hold during operation. This means that, namely, the node pairs exchanging traffic are the same, only shortest path routing is utilized, only the minimum number of 3Rs required for signal regeneration can be used (although in any feasible combination of nodes, dependent on the network state), and the path computation metric is distance.

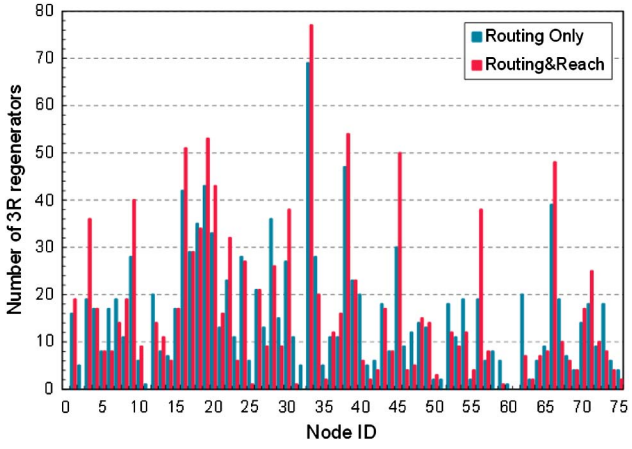

Fig. 6. Distribution of 3R regenerators for $r_{3R} = 0.12$ using the routing only and routing and reach strategies.

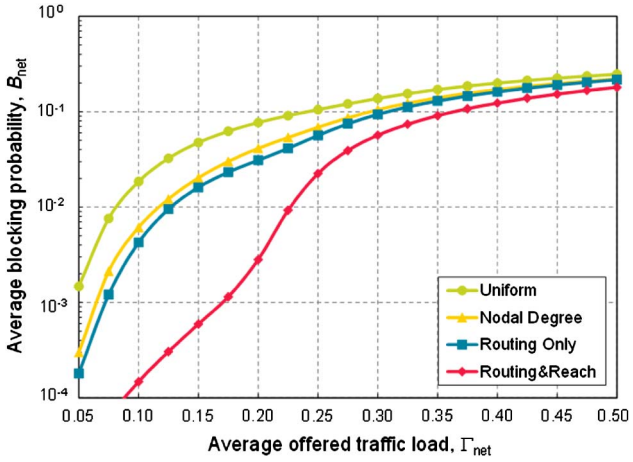

Fig. 7. Service blocking performance for $r_{3R} = 0.08$ with matching planning and operation conditions.

The plot in Fig. 7 shows the blocking performance as a function of the average offered traffic load for $r_{3R} = 0.08$ and using the four fitness computation strategies. As can be seen, employing a strategy that embeds more information when computing fitness enables, during network operation, the number of services blocked due to lack of regenerator resources to be significantly decreased. Notably, a first improvement is evident just by considering the nodal degree; then, to a lesser extent, another reduction of blocking when taking into account how demands are expected to be routed; and, finally, a substantial performance improvement when the most likely nodes for 3R placement along each routing path are also used as input.

Figure 8 presents the blocking performance as a function of the normalized 3R regenerator count for $\Gamma_{net} = 0.20$. A common trend to all strategies is that increasing the total number of predeployed regenerators decreases the average blocking probability, but only up to reaching a performance

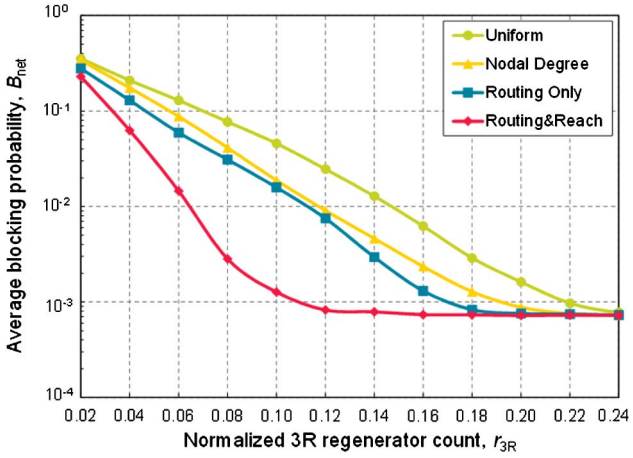

Fig. 8. Service blocking performance for $\Gamma_{net} = 0.20$ with matching planning and operation conditions.

boundary that corresponds to having the majority of service blocking events from the lack of free wavelength resources and not regenerators. Importantly, this plot highlights the benefit, in terms of the smaller number of 3R regenerators needed to attain the performance boundary, from exploiting more information in the regenerator predeployment. For instance, minimizing blocking requires a regenerator count of 24% if the uniform strategy is used. This figure drops to around 20% if the nodal degree strategy is used instead and to 18% with routing only. Still, the highest regenerator savings are achieved with the routing and reach strategy, enabling this optimum value to be reduced to only 12%.

C. Mismatches Between Planning and Operation

The simulation results with matching conditions during planning and operation clearly support the effectiveness of embedding more information into the fitness computation process. However, due to different factors, the conditions of operation of the DWDM network may differ from the ones assumed at the planning stage. In the following, some of the main planning assumptions are challenged during network operation, and the impact on the performance provided by the fitness estimation strategies is investigated.

Figure 9 plots the blocking performance as a function of the normalized 3R regenerator count for $\Gamma_{\text{net}} = 0.20$ and assuming a different routing path algorithm is employed during network operation. More precisely, instead of using the shortest distance path considered when planning the predeployed 3R regenerators, fixed alternate routing with the three shortest distance paths is utilized when routing the traffic demands during network operation. As can be seen, the results exhibit a similar relative behavior to that observed when the same routing algorithm is used in both planning and operation, that is, the fitness computation strategies exploiting more information enable lower service blocking and a smaller number of 3R regenerators for a target blocking probability. This is due to the evidence that, although the longer routing paths are being used in operation when the shortest one is not available, most of the wavelength services are still being routed over the shortest distance path, which is the one considered by the routing only and routing and reach strategies.

A potentially more impacting mismatch consists of using a different path computation metric in operation from that assumed in planning. Therefore, considering that, instead of the distance metric utilized in planning, traffic demands are actually routed over the shortest path in number of hops, Figs. 10 and 11 present the service blocking performance for $r_{3R} = 0.08$ and $\Gamma_{\text{net}} = 0.20$, respectively. The simulation results show a general increase in service blocking with all fitness computation strategies, which is attributed to the fact that for some node pairs the shortest hop count path requires more 3R regenerators than its distance based counterpart. However, it can also be observed that with routing only and routing and reach strategies the blocking performance degradation is larger. In fact, in some of the cases depicted, using these strategies can even lead to

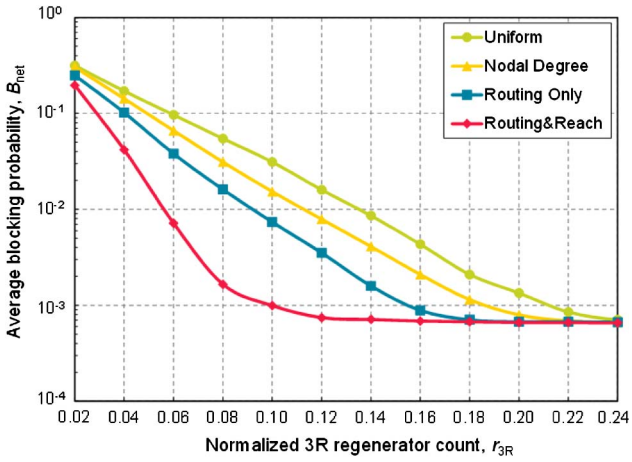

Fig. 9. Service blocking performance for $\Gamma_{\text{net}} = 0.20$ with mismatch of the routing algorithm used in planning and operation.

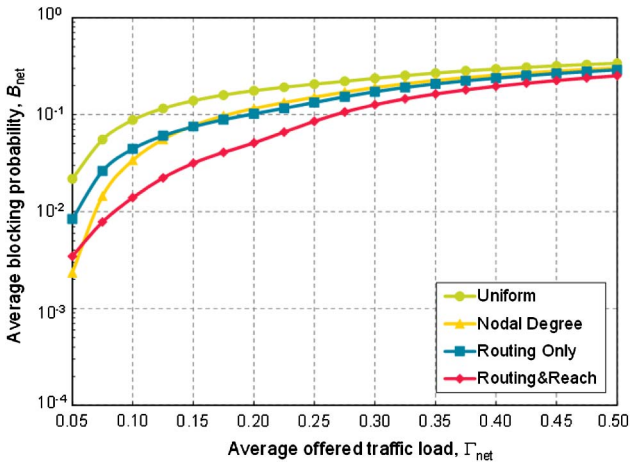

Fig. 10. Service blocking performance for $r_{3R} = 0.08$ with mismatch of the path computation metric used in planning and operation.

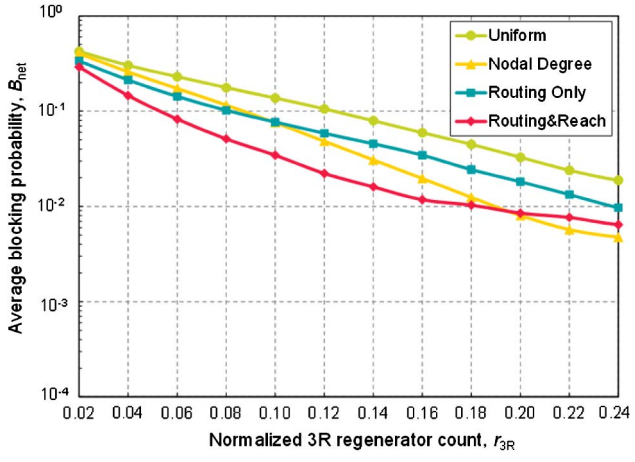

Fig. 11. Service blocking performance for $\Gamma_{\text{net}} = 0.20$ with mismatch of the path computation metric used in planning and operation.

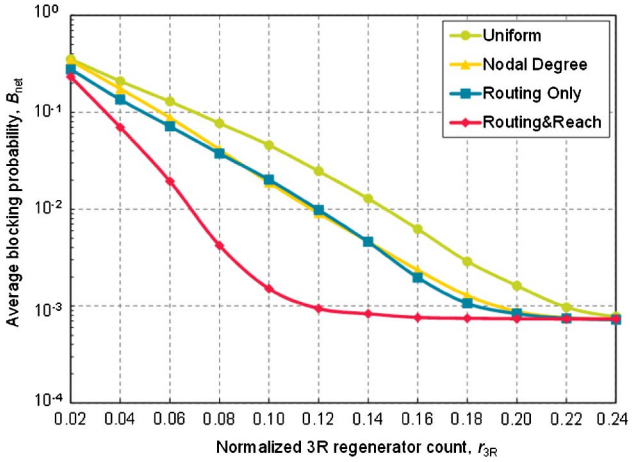

Fig. 12. Service blocking performance for $\Gamma_{net} = 0.20$ with mismatch of the traffic pattern used in planning and operation.

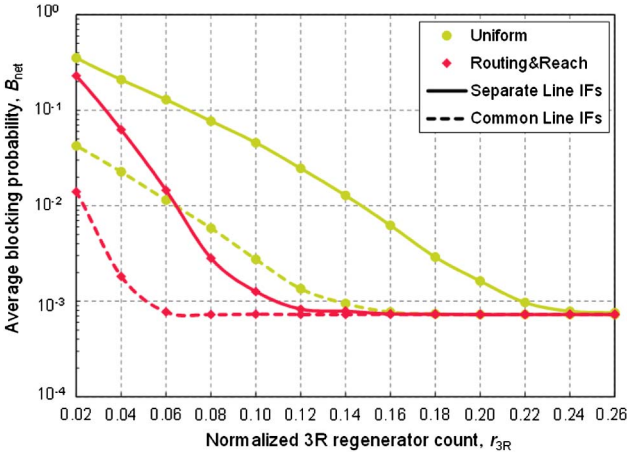

Fig. 13. Service blocking performance for $\Gamma_{net} = 0.20$ and common versus separate line interfaces.

higher service blocking than with the simpler nodal degree, which in turn again outperforms the uniform strategy. As a result, it can be concluded that if the routing paths most used during network operation differ significantly from the ones that have been assumed in planning, the effectiveness of the fitness computation strategies that exploit this information can be compromised. Nevertheless, in the cases shown, the routing and reach strategy still provided better performance than routing only.

In the last mismatch scenario considered, it is assumed that during network planning no information is available regarding which node pairs will exchange traffic when the network starts to operate. In this circumstance, the routing only and routing and reach strategies are applied assuming all node pairs are equally likely to exchange traffic. The resulting blocking performance for $\Gamma_{net} = 0.20$ is presented in Fig. 12. The simulation results show that there is a small performance degradation with both strategies that exploit routing path information. Although small, this additional blocking penalty is enough to prevent the routing only strategy from providing any relevant advantage over the simpler nodal degree.

D. Common Line Interfaces for Transponders and Regenerators

As discussed, the deployment of node architectures with an ODU switch between client and line interfaces is expected to provide a better utilization of the line interface resources in a dynamic service provisioning scenario. In order to gain insight into the order of magnitude of such improvements, the final set of simulation compares the service blocking performance with common and separate line interfaces. In particular, Fig. 13 plots the blocking performance assuming $r_{TP} = 0.10$, r_{3R} between 0.02 and 0.26, $\Gamma_{net} = 0.20$, matching of planning and operation conditions, and two strategies for fitness computation: uniform and routing and reach. Line interfaces are either kept separate for transponders and regenerators or are common for both functionalities.

The simulation results support two main trends. The first one is that the effectiveness of embedding more information into fitness computation is preserved with common line interfaces. In fact, with the uniform strategy a regenerator count of around 16% is required to minimize the blocking probability, whereas this figure drops to around half (8%) when the routing and reach strategy is used instead. The second trend supported by the simulation results is that sharing the line interfaces for transponder and regenerator functionalities significantly enhances their utilization. As can be observed, with the uniform strategy the regenerator count needed to minimize blocking is decreased from around 24% to 16% by having common line interfaces instead of separate ones. Moreover, with the routing and reach strategy the equivalent figures are of around 14% and 8%.

IV. Conclusion

This paper proposed a stochastic-based framework for predeploying a set of 3R regenerators in long-haul DWDM networks designed to support fast wavelength service provisioning. Four strategies were described to determine the fitness of each network node as a placeholder for 3R regenerators and a heuristic algorithm to deploy the 3R regenerators as to match as close as possible their fitness values was presented. Network simulation was utilized to assess the performance of the four fitness computation strategies in different scenarios regarding the traffic pattern, routing algorithm, and path computation metric forecasted during network planning and the ones enforced during network operation. The comprehensive analysis highlighted, on the one hand, the importance of exploiting more information when predeploying 3R regenerators as a way to enhance the success ratio of service setup and reduce the number of predeployed regenerators and, on the other hand, how the extent of these improvements depends on which of the assumptions made during network planning do not hold during network operation. Particularly, the results obtained suggest that the fitness computation strategies embedding routing and optical performance

information only become clearly less effective when the routing paths assumed at the planning stage are significantly different from the ones utilized during network operation. The results also support that in the absence of reliable routing path information during planning the more efficient strategy is to distribute these devices proportionally to the nodal degree. Moreover, the last set of simulation results presented emphasizes the benefit of using common line interfaces to realize both the transponder and regenerator functionalities.

Future work may include imposing a larger mismatch between the traffic pattern assumed in planning and the one observed in operation, limiting the number of nodes where 3R regenerators can be predeployed, and devising more advanced strategies for fitness computing (e.g., adding a residual fitness value dimensioned via the nodal degree to the strategies using routing and reach information).

Appendix A

The MILP model to minimize the deviation between the estimated and actual distribution of the 3R regenerators is described below.

Objective function:

$$\min \sum_{i=1}^{N} x_{3R}(i). \tag{A1}$$

Constraints:

$$x_{3R}(i) \geq \mathrm{pdf}_{3R}(i) - n_{3R}(i)/n_{3R}^{\mathrm{total}}, \qquad 1 \leq i \leq N, \tag{A2}$$

$$x_{3R}(i) \geq n_{3R}(i)/n_{3R}^{\mathrm{total}} - \mathrm{pdf}_{3R}(i), \qquad 1 \leq i \leq N, \tag{A3}$$

$$2 \cdot n_{3R}(i) + n_{\mathrm{TP}}(i) \leq n_{\mathrm{AD}}(i), \qquad 1 \leq i \leq N, \tag{A4}$$

$$\sum_{i=1}^{N} x_{3R}(i) = n_{3R}^{\mathrm{total}}, \tag{A5}$$

$$n_{3R}(i) \in \mathbb{N}_0, \qquad 1 \leq i \leq N. \tag{A6}$$

The objective function, Eq. (A1), minimizes the sum of the differences between the expected regenerator PDF and the one obtained from dividing the number of 3R regenerators deployed at the node by the total number of predeployed regenerators. Constraints (A2) and (A3) are used to model both the case where the expected PDF exceeds the actual one and the case where the opposite occurs. Moreover, constraint (A4) guarantees that at each node i the maximum add/drop port capacity is verified, assuming the number of predeployed transponders, $n_{\mathrm{TP}}(i)$, is already known, whereas constraint (A5) imposes that exactly n_{3R}^{total} regenerators are assigned to the network nodes. Finally, (A6) enforces that variables $n_{3R}(i)$ only assume integer values.

Both the abovementioned MILP model and the heuristic algorithm of Section II were used to minimize the 3R fitness deviation in a smaller 24-node US network topology [2]. For different total numbers of 3R regenerators, n_{3R}^{total}, both approaches always returned the same value of the objective function, suggesting that the devised heuristic algorithm can efficiently perform the task of distributing the 3R regenerators by the network nodes as to match as close as possible their fitness values.

References

[1] S. Gringeri, B. Basch, V. Shukla, R. Egorov, and T. Xia, "Flexible architectures for optical transport nodes and networks," *IEEE Commun. Mag.*, vol. 48, no. 7, pp. 40–50, July 2010.

[2] A. Eira, J. Pedro, and J. Pires, "Optimized design of fixed/flex-rate line-cards and transceivers over multiple planning cycles," in *Optical Fiber Communication Conf. (OFC)*, San Francisco, CA, 2014, paper W2A.47.

[3] A. Félix, N. Borges, H. Wu, M. Hanlon, M. Birk, and A. Tschersich, "Multi-layer SDN on a commercial network control platform for packet optical networks," in *Optical Fiber Communication Conf. (OFC)*, San Francisco, CA, 2014, paper Th5A.1.

[4] J. Pedro and S. Pato, "Impact of add/drop port utilization flexibility in DWDM networks [Invited]," *J. Opt. Commun. Netw.*, vol. 4, pp. B142–B150, Nov. 2012.

[5] S. Woodward, M. Feuer, K. Inwoong, P. Palacharla, X. Wang, and D. Bihon, "Service velocity: Rapid provisioning strategies in optical ROADM networks," *J. Opt. Commun. Netw.*, vol. 4, pp. 92–98, Feb. 2012.

[6] F. Rambach, B. Konrad, L. Dembeck, U. Gebhard, M. Gunkel, M. Quagliotti, L. Serra, and V. López, "A multilayer cost model for metro/core networks," *J. Opt. Commun. Netw.*, vol. 5, pp. 210–225, Mar. 2013.

[7] R. Morais, J. Pedro, P. Monteiro, and A. Pinto, "Impact of node architecture in the power consumption and footprint requirements of optical transport networks," *J. Opt. Commun. Netw.*, vol. 5, pp. 421–436, May 2013.

[8] S. Kim, S. Seo, and S. Kim, "Regenerator placement algorithms for connection establishment in all-optical networks," in *Proc. IEEE GLOBECOM*, San Francisco, CA, 2000, vol. 2, pp. 1205–1209.

[9] A. Patel, C. Gao, J. Jue, X. Wang, Q. Zhang, P. Palacharla, and T. Naito, "Optimal traffic grooming and regenerator placement in WDM optical networks," in *Optical Fiber Communication Conf. (OFC)*, San Diego, CA, 2010, paper NTuA1.

[10] X. Yang and B. Ramamurthy, "Sparse regeneration in translucent wavelength-routed optical networks: Architecture, network design and wavelength routing," *Photon. Netw. Commun.*, vol. 10, no. 1, pp. 39–53, July 2005.

[11] B. Bathula, R. Sinha, A. Chiu, M. Feuer, G. Li, S. Woodward, W. Zhang, R. Doverspike, P. Magill, and K. Bergman, "Constraint routing and regenerator site concentration in ROADM networks," *J. Opt. Commun. Netw.*, vol. 5, no. 11, pp. 1202–1214, Nov. 2013.

[12] N. Barakat and A. Leon-Garcia, "An analytical model for predicting the locations and frequencies of 3R regenerations in all-optical wavelength-routed WDM networks," in *Proc. IEEE ICC*, New York, 2002, vol. 5, pp. 2812–2816.

[13] R. Skoog and B. Wilson, "Transponder pool sizing in highly dynamic translucent WDM optical networks," in *Optical Fiber Communication Conf. (OFC)*, San Diego, CA, 2010, paper NTuA3.

[14] J. Pedro, "Pre-deployment of regenerators in DWDM networks and the impact of mismatches between planning and operation," in *Optical Fiber Communication Conf. (OFC)*, San Francisco, CA, 2014, paper M2B.2.

[15] J. Pedro, J. Santos, and R. Morais, "Dynamic setup of multi-granular services over next-generation OTN/DWDM networks: Blocking versus add/drop port usage," in *IEEE Int. Conf. on Transparent Optical Networks (ICTON)*, 2012, paper Tu.B1.5.

[16] "DARPA Core Optical Networks (CORONET) Continental United States (CONUS) topology" [Online]. Available: http://monarchna.com/CORONET_CONUS_Topology.xls.

João Pedro (M'11) was born in Lisboa, Portugal, and received his M.Sc. and Ph.D. degrees in electrical and computer engineering from Instituto Superior Técnico (IST), Lisbon Technical University, Lisboa, Portugal, in 2004 and 2011, respectively.

He was a research engineer and a system architect for network planning tools at Nokia Siemens Networks (NSN) Portugal S.A., Amadora, Portugal, in the periods between 2008 and 2010 and 2010 and 2013, respectively. Since 2013 he has been with Coriant Portugal, Unipessoal Lda, Amadora, Portugal, leading the research activities in network optimization and supporting the design of algorithms for the network planning tools. He has authored or co-authored over 100 publications in international conferences and journals and participated in the EU FP7 Integrated Projects FUTON and IDEALIST. He has also been a lecturer of courses on network planning and transport networks at IST and Instituto Superior de Transportes e Comunicações (ISUTC), Mozambique. Currently, his research interests include routing and spectrum assignment algorithms, optical node architectures, circuit switched transport networks, multilayer optimization, and advanced optical networking paradigms (burst/packet switching).

Dr. Pedro is a member of IEEE and a collaborator of the Instituto de Telecomunicações (IT), Lisboa, Portugal.